Soft Matter

Accepted Manuscript

ROYAL SOCIETY OF CHEMISTRY

www.rsc.org/softmatter

Combined effects of underlying substrate and evaporative cooling on the evaporation of sessile liquid droplets

Yilin Wang, [a] Liran Ma, [b] Xuefeng Xu*[a] and Jianbin Luo [b]

[a] *School of Technology, Beijing Forestry University, Beijing 100083, China*

[b] *State Key Laboratory of Tribology, Tsinghua University, Beijing 100084, China*

Abstract

The evaporation of pinned, sessile droplets resting on finite thickness substrates is investigated numerically by extending the combined field approach to include the thermal properties of the substrate. By using the approach, the combined effects of the underlying substrate and the evaporative cooling are characterized. The results show that the influence of the substrate on the droplet evaporation depends largely on the strength of the evaporative cooling. When the evaporative cooling is weak, the influence of substrate is also weak. As the strength of evaporative cooling increases, the influence of the substrate becomes more and more pronounced. Further analyses indicate that it is the cooling at the droplet surface and the temperature dependence of the saturation vapor concentration that relate the droplet evaporation to the underlying substrate. This implies that the evaporative cooling number ***Ec*** can be used to identify the influence of the substrate on the droplet evaporation. The theoretical predictions by the present model are compared and found in good agreement with the experimental measurements. The present work may contribute to the body of knowledge concerning droplet evaporation and may have applications in a wide range of industrial and scientific processes.

Keywords: Droplet; Substrate; Evaporative cooling; Combined field approach.

* Corresponding author. E-mail: xuxuefeng@bjfu.edu.cn

Ⅰ. Introduction

When a liquid droplet dries out, the particles suspended inside the droplet will be left on the underlying substrate and form different deposits patterns, e.g., a ring deposit, a center deposit, and a uniform deposit [1-6]. Predicting and controlling the deposition pattern is of vital importance in many industrial and scientific applications such as ink-jet printing of functional materials [7-9], disease diagnosis [10] and automatic DNA mapping [11,12]. The evaporation of sessile droplet has significant influences on the evaporation-induced particle deposition, and thus has attracted extensive attention in recent years [13-27].

For the quasi-steady diffusion-limited evaporation, the vapor concentration in the atmosphere satisfies Laplace's equation [28,29]. Assuming that the atmosphere just above the droplet surface is saturated with vapor and that the vapor concentration is constant along the surface (referred to as the "isothermal model" in the following), Picknett and Bexon [30], Deegan et al. [3,31], and Popov [32] derived an exact solution for the evaporation flux along the surface of pinned sessile droplets. They showed that the evaporation increases monotonically from the droplet center to the droplet edge and diverges at the contact line.

Using a finite-element method, Hu and Larson [29,33,34] obtained a simple, yet accurate empirical expression for the evaporation flux of sessile droplets. This analytical expression for the evaporation flux is then used as a boundary condition to compute the temperature field inside drying droplets [35]. The results showed that the nonuniform evaporation lead to a nonuniform distribution of temperature along the droplet surface and the surface temperature gradient reverses its direction at a critical contact angle. Ristenpart et al. [36] and Xu et al. [28] indicated that the critical contact angle depends on the thermal conductivity and the thickness of the substrate. Girard et al. [14,37] further pointed out that both the temperature of the substrate and the size of the heating zone have significant influences on the evaporation of sessile droplets.

The decrease in the liquid temperature at the droplet surface will lower the vapor saturation concentration there, and will in turn reduce the evaporation of the droplet [17,18,35,38-43]. Experiments conducted on super-hydrophobic substrates by Dash and Garimella [44] indicated that the "isothermal model" overpredicts the evaporation rate of drying droplets by ~20%. This deviation is confirmed by the numerical simulations by Pan et al. [45,46], who attributed the discrepancy to the large temperature reduction at the droplet surface due to the thermal resistance of the relatively tall droplet on a superhydrophobic substrate. Reducing the atmosphere pressure will enhance evaporation and thus highlight the temperature reduction. For water droplets drying in an atmosphere of helium at a pressure of around 40 mbar, the evaporation rate is as low as 20% of the one predicted by the "isothermal model" [18,47].

Allowing the saturation concentration of vapor to be a function of the local liquid temperature rather than simply a constant, Dunn et al. [38-40], Sefiane et al. [18] and Saada et al. [41] generalized the basic isothermal model to include the effect of the evaporative cooling. Taking into account the thermal effects resulting from evaporative cooling, Sefiane and Bennacer [47-49] developed a theoretical expression for the evaporation rate of sessile droplets and introduced a dimensionless number ***SB***, which relates substrate and liquid properties as well as the evaporation kinetics, to identify the threshold for the transition from an isothermal case to a nonisothermal one. Their theory is supported by a very wide range of experimental measurements. Developing a combined field approach which unifies the coupled fields in liquid evaporation into one single field and makes the iteration unnecessary, Xu and Ma [50] numerically investigated the influence of evaporative cooling on the evaporation of sessile droplets resting on an isothermal substrate. They derived a dimensionless number ***Ec*** to evaluate the strength of the evaporative cooling. Their results showed that a critical value $\boldsymbol{Ec}_{\mathbf{Crit}}$ exists below which the evaporative cooling effect can be neglected and above which the significance of the effect increases

dramatically. Good agreement is found between their theoretical predictions and the experimental measurements without any parameter fitting.

In the basic isothermal model, the substrate has no effect on the droplet evaporation due to the assumption of the constant vapor concentration along the surface. This means that the same droplets must have the same evaporation rate on any kind of substrates. However, for a sessile droplet in contact with a surface, the underlying substrate must have impacts on the liquid evaporation. Saada et al. [41] indicated that the evaporation rate of sessile droplets varies significantly with the substrate and is higher for substrates with higher thermal conductivity or smaller thickness. Sefiane et al. [18,38-40,43,47] experimentally investigated the evaporation rates of sessile droplets of different liquids in atmospheres of various ambient gases at different pressures using different substrates with a wide range of thermal conductivities. They also found that the evaporation rate of sessile droplets can be influenced by the thermal properties of substrate and that the evaporative cooling is more pronounced on the substrate with lower thermal conductivity. They explained the behaviors by introducing a mathematical model for the droplet evaporation including the variation of the saturation concentration with temperature. Semenov et al. [51] numerically obtained the dependences of the average surface temperature of sessile droplets on the substrate thermal conductivity and the substrate temperature, and then investigated the influences of substrate thermal properties on the droplet evaporation by using the calculated average surface temperature.

Because the vapor diffusion in the atmosphere and the heat transfer in the liquid and the substrate are coupled, the influence of the substrate on the droplet evaporation should be closely related with the evaporative cooling. However, despite notable progress over the past few decades, a full understanding for the combined effects of the underlying substrate and the evaporative cooling on the droplet evaporation is still not achieved and quantitative studies are still needed. In this paper, the combined field approach for the droplet evaporation [50] is first extended to include the thermal properties of the underlying substrates. The present approach is validated by comparison with the experimental

measurements. Then, by using the approach, the evaporation of sessile droplets of various liquids with a wide range of evaporative cooling number ***Ec*** on substrates with a wide range of thermal conductivities, thickness, and temperature is solved numerically, and how the evaporative cooling affects the influences of substrate properties on the droplet evaporation is analyzed quantitatively. The present work may contribute to the body of knowledge concerning the droplet evaporation and will be useful to control the deposition pattern of drying droplets.

Ⅱ. Mathematic Model

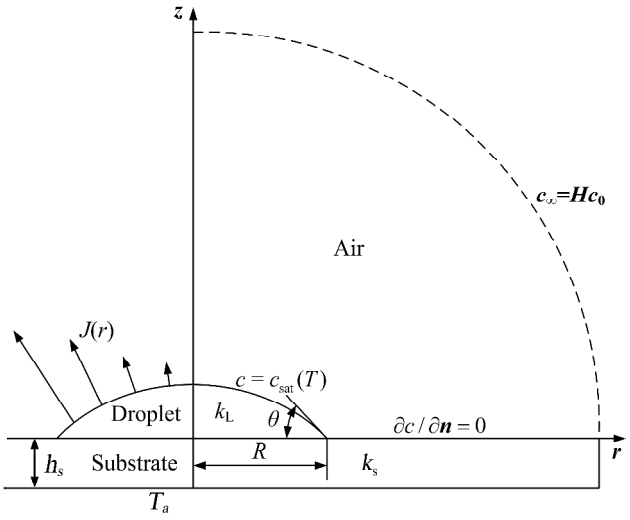

FIG 1 A sessile spherical-cap droplet resting on a flat substrate in a cylindrical coordinate system with radial coordinate r and axial coordinate z.

Here, we consider a small, pinned, and slowly evaporating liquid droplet with a contact angle of θ and contact line radius of R resting on a flat substrate of thickness h_S (Fig. 1). The thermal conductivities of the substrate and the liquid are k_S and k_L, respectively. The temperature at the lower surface of the substrate is fixed at T_a and the room temperature is T_0. Since the Bond number and the capillary number are small, the droplet shape can be regarded as a spherical cap.

By estimating the ratio of the relative rates of change of droplet height to that of temperature, Hu and Larson [35] showed that the transient in the energy equation for droplet evaporation can be neglected. Under such a quasi-steady condition, the heat equation in the droplet is $\mathbf{Pe}\,\boldsymbol{u}\cdot\nabla T+\nabla^2 T=0$, where $\boldsymbol{u}$ is

the liquid velocity, and the Peclet number **Pe** is a ratio of the convective to the conductive heat transfer [36]. Typically $\mathbf{Pe} \ll 1$, implying that the rate of the convective heat transfer is much smaller than that of the conductive one in the droplets [35,36]. Ristenpart et al. [36] further indicated that, although the velocity $\boldsymbol{u}$ diverges in the vicinity of the contact line, conduction is nonetheless dominant in the whole droplet. Assuming that the air is quiescent, vapor transport in the air is solely by diffusion. Hu and Larson [29,34] indicated that the vapor concentration adjusts rapidly compared to the time required for droplet evaporation and can thus be considered to be at a quasi-steady state. Therefore, for the quasi-steady diffusion-limited evaporation, the concentration of vapor c in the atmosphere, the temperature T_L in the liquid, and the temperature T_S in the substrate all satisfy Laplace's equation, i.e., $\nabla^2 c = 0$, $\nabla^2 T_L = 0$ and $\nabla^2 T_S = 0$ [15,16,28,29,33]. According to the combined field approach [50], these Laplace's equations and the boundary conditions in the droplet evaporation can be rewritten in a dimensionless form as:

$$\tilde{\nabla}^2 \tilde{T}_1 = 0 \quad \text{for} \quad \tilde{z} \geq \tilde{h}(\tilde{r}) \tag{1}$$

$$\tilde{\nabla}^2 \tilde{T}_2 = 0 \quad \text{for} \quad 0 \leq \tilde{z} \leq \tilde{h}(\tilde{r}),\ \tilde{r} \leq 1 \tag{2}$$

$$\tilde{\nabla}^2 \tilde{T}_3 = 0 \quad \text{for} \quad -h_R \leq \tilde{z} \leq 0 \tag{3}$$

$$\tilde{T}_1 = -1 \quad \text{for} \quad \tilde{z} = \infty,\ \tilde{r} = \infty \tag{4}$$

$$\tilde{T}_1 = \tilde{T}_2,\ \ \boldsymbol{Ec}\frac{\partial \tilde{T}_1}{\partial \boldsymbol{n}} = \frac{\partial \tilde{T}_2}{\partial \boldsymbol{n}} \quad \text{for} \quad \tilde{z} = \tilde{h}(\tilde{r}), \tilde{r} \leq 1 \tag{5}$$

$$\tilde{T}_2 = \tilde{T}_3,\ \ \frac{\partial \tilde{T}_2}{\partial \boldsymbol{n}} = \boldsymbol{k_R}\frac{\partial \tilde{T}_3}{\partial \boldsymbol{n}} \quad \text{for} \quad \tilde{z} = 0,\ \ \tilde{r} \leq 1 \tag{6}$$

$$\tilde{T}_3 = \tilde{T}_a \quad \text{for} \quad \tilde{z} = -h_R \tag{7}$$

$$\frac{\partial \tilde{T}_3}{\partial \boldsymbol{n}} = 0 \quad \text{for} \quad -h_R \leq \tilde{z} \leq 0,\ \ \tilde{r} = \infty \tag{8}$$

$$\frac{\partial \tilde{T}_1}{\partial \boldsymbol{n}} = 0, \frac{\partial \tilde{T}_3}{\partial \boldsymbol{n}} = 0, \text{ for } \ \tilde{r} > 1,\ \ \tilde{z} = 0 \tag{9}$$

Where $\tilde{\nabla}^2=\frac{\partial^2}{\partial^2\tilde{r}}+\frac{1}{\tilde{r}}\frac{\partial}{\partial\tilde{r}}+\frac{\partial^2}{\partial^2\tilde{z}}$, $\tilde{r}=\frac{r}{R}$, $\tilde{z}=\frac{z}{R}$, $\tilde{h}(\tilde{r})=h(r)/R$, $\tilde{T}_1=\frac{c-c_0}{c_0(1-H)}$, $\tilde{T}_2=\frac{b(T_L-T_0)}{c_0(1-H)}$,

$\tilde{T}_3=\frac{b(T_S-T_0)}{c_0(1-H)}$, $\tilde{T}_a=\frac{b(T_a-T_0)}{c_0(1-H)}$, $c_0=c_{\mathrm{sat}}(T_0)$, $b=\frac{dc_{sat}}{dT}\Big|_{T=T_0}$, $\boldsymbol{Ec}=\frac{H_L Db}{k_L}$, $\boldsymbol{h_R}=h_s/R$, $\boldsymbol{k_R}=k_S/k_L$,

$h(r)$ is the droplet height, H is the relative humidity of the ambient air, H_L is the latent heat of evaporation, D is the coefficient of diffusion of vapor in the atmosphere, and $\boldsymbol{n}$ is the unit normal.

Here, ***Ec*** is the evaporative cooling number which characterizes the ratio of the reduction in the evaporation flux due to cooling to its isothermal value and can be used to estimate the intensity of the evaporative cooling. The larger the value of ***Ec***, the more significant the negative feedback effect of evaporative cooling which reduces the evaporation rate. Its definition implies that the value of the number ***Ec*** is determined only by the thermal properties of the liquid and the atmosphere. Under a temperature of 295 K and an atmospheric pressure of 99.8 kPa, ***Ec*** are 0.11, 0.84 and 1.03 for water, methanol and acetone in the air, respectively, and are 0.37, 3.34 and 4.13 for water, methanol and acetone in the helium, respectively [50].

If we consider $\tilde{T}_1$, $\tilde{T}_2$, and $\tilde{T}_3$ as the temperature in the air, in the liquid and in the substrate respectively, the above equations (1-9) represent a heat conduction field in the surrounding air with thermal conductivity of ***Ec***, in the liquid droplet with thermal conductivity of 1, and in the substrate with thermal conductivity of k_R. As a result, the coupled fields in the droplet evaporation, i.e., the vapor concentration field in the surrounding atmosphere, the temperature field in the liquid, and the temperature field in the substrate, have been combined into one "quasi-temperature" field, and therefore, $\tilde{T}_1$, $\tilde{T}_2$, and $\tilde{T}_3$ can be numerically solved without the iterative schemes. Once $\tilde{T}_1$, $\tilde{T}_2$, and $\tilde{T}_3$ are known, the temperature in the droplet and in the substrate, the vapor concentration in the atmosphere, and the evaporation flux from the droplet surface can be easily computed.

The dimensionless equations (1-9) clearly indicate that, the evaporation of sessile droplet resting on finite thickness substrates is governed by five dimensionless numbers: ***Ec***, θ, k_R, h_R, and $\tilde{T}_a$. The number ***Ec*** characterizes the strength of the evaporative cooling and its value is determined only by the thermal properties of the liquid and the atmosphere [50]. The contact angle θ indicates the spatial configuration of the droplet. For a liquid droplet with given geometry and given thermal properties, its evaporation is only governed by k_R, h_R, and $\tilde{T}_a$, which are the relative thermal conductivity, the relative thickness, and the dimensionless temperature of the substrate respectively. To analyze the effects of these substrate properties on the droplet evaporation and the influences of the evaporative cooling on the effects of the substrate, the above dimensionless equations are numerically solved by using a commercial software, ANSYS (Ansys, Inc).

Ⅲ. Results and Discussion

A. Effects of the substrate thermal conductivity.

The evaporation of sessile droplets of various liquids with a wide range of ***Ec*** on substrates with a wide range of K_R is calculated to investigate the effects of the substrate thermal conductivity on the droplet evaporation and the influences of the evaporative cooling on these effects.

First, the dimensionless evaporation flux $\tilde{J}(\tilde{r}) = -\tilde{\nabla}\tilde{\boldsymbol{T}}_1 \cdot \boldsymbol{n} = \dfrac{J(r)R}{Dc_0(1-H)}$, where $J(r) = -D\nabla c \cdot \boldsymbol{n}$ is the evaporation flux along the surface of the sessile droplet, is illustrated as a function of $\tilde{r}$ in Fig. 2. From the figure it can be seen that the evaporation flux always increases monotonically along the droplet surface from the droplet center to the droplet edge, and becomes infinite as r approaches the contact line. This distribution trend is same for all kinds of substrates, and is consistent with the previous theoretical and numerical results [3,29,30]. The figure also demonstrates the significant influence of the substrate thermal conductivity: the larger the value of k_R, the higher the evaporation flux from the droplet surface, and the more pronounced the increase in the evaporation flux towards the contact line.

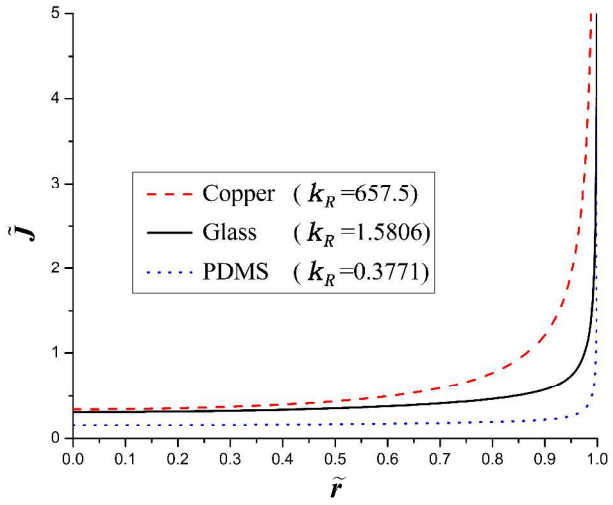

FIG 2 The dimensionless evaporation flux $\tilde{J}$ along the surface of drying water droplets at contact angles of 10º computed by the finite element method. Here, the parameters are chosen as follows: h_R=0.15, ***Ec***=10, $\tilde{T}_a = 0$, k_L =0.60988 $wk^{-1}m^{-1}$ for water, k_S = 401 $wk^{-1}m^{-1}$, 0.96 $wk^{-1}m^{-1}$, and 0.23 $wk^{-1}m^{-1}$ for copper, glass, and PDMS respectively, and the relative thermal conductivities k_R = 657.5, 1.5806, and 0.3771 for the substrates of copper, glass, and PDMS respectively.

Fig. 3 further indicates that the effects of the substrate thermal conductivity on the droplet evaporation depend on the strength of the evaporative cooling. When ***Ec*** is close to zero, the evaporation rates on all substrates with different thermal conductivities are almost the same. This means that, in the case the evaporative cooling effect is weak, the substrate thermal conductivity has also weak influence on the droplet evaporation. From Fig. 3 it can be seen that, when ***Ec*** is less than 0.2, the relative difference in the evaporation rate between droplets on a perfect thermal insulating substrate (e.g., PDMS) and droplets on a perfect thermal conducting substrate (e.g., copper) is not more than 9%.

Fig. 3 also shows that, as the strength of evaporative cooling increases, the evaporation rate of the droplets continues to decrease and the influence of the substrate thermal conductivity becomes more and more significant. The decrease in the evaporation rate of droplets is more pronounced on the substrate of poor thermal conductor and less pronounced on the substrate of good thermal conductor, and thus droplets on a substrate with higher thermal conductivity will yield a higher evaporation rate when the

evaporative cooling effect is notable. We can read from the figure that the evaporation rate on a perfect thermal conducting substrate (namely, copper) is almost double to that on a perfect thermal insulating substrate (namely, PDMS) when ***Ec*** =2.

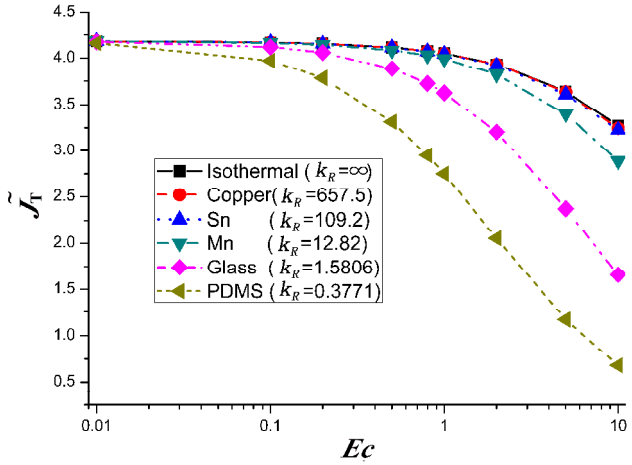

FIG 3 The dimensionless total evaporation rate over the whole surface of sessile droplets at contact angles of 10º computed by the finite element method. The parameters used are as follows: h_R= 0.15, $\tilde{T}_a = 0$.

The variations of evaporation rate with k_R for different values of ***Ec*** can illustrate more clearly the influence of the evaporative cooling on the effect of the substrate thermal conductivity on the droplet evaporation. From Fig. 4a it can be easily seen that the decrease in the evaporation rate with decreasing substrate thermal conductivity is closely related to the strength of evaporative cooling. The decrease is more pronounced for the case that the evaporative cooling is stronger. Here, we define $k_{R,0.95}$ as the relative thermal conductivity of substrate at which the evaporation rate reduces to 95% of the rate for infinite thermal conductivity. The values of $k_{R,0.95}$ have been measured from Fig. 4a and been plotted against ***Ec*** in Fig. 4b. The numerical results show that $k_{R,0.95}$ increases almost linearly with increasing ***Ec***. In the special case in which there is no evaporative cooling, corresponding to ***Ec***=0, $k_{R,0.95}$ also reduces to zero. This indicates that even a perfect thermal insulating substrate will have no influence on the droplet evaporation if the effect of evaporative cooling can be neglected.

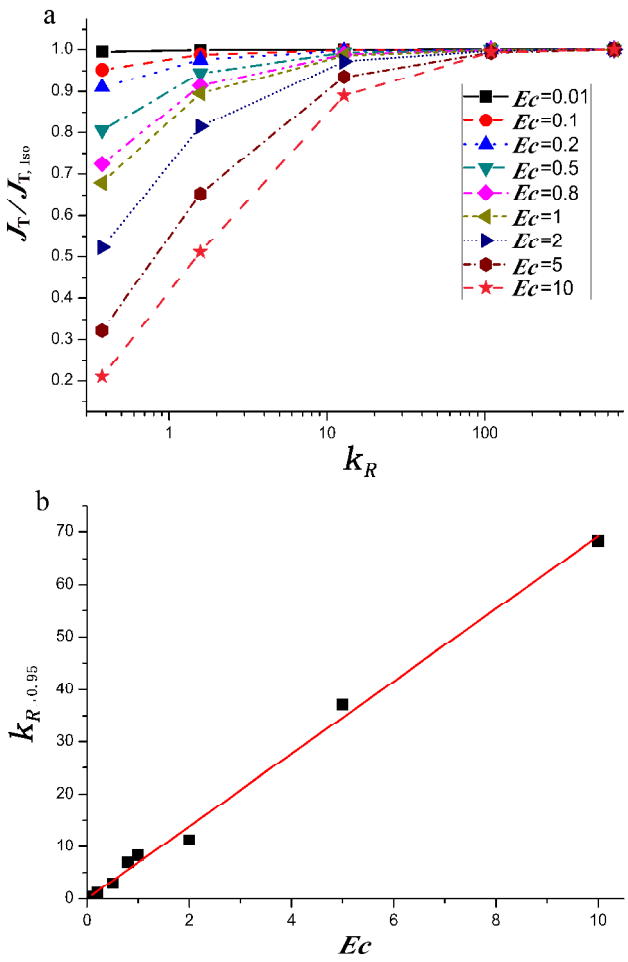

FIG 4 (a) The relative total evaporation rate of sessile droplets $J_T/J_{T,Iso}$. Here, $J_{T,Iso}$ is the total evaporation rate for isothermal substrates (i.e., $k_R=\infty$). (b) $k_{R,0.95}$ *versus* $\boldsymbol{Ec}$. The solid squares are from numerical calculations, and the solid line is the best linear fit through zero to the numerical data and yields $k_{R,0.95} = 6.92392\boldsymbol{Ec}$.

B. Effects of the substrate thickness

Since the evaporation of sessile droplets is shown to be dependent on the thermal conductivity of the underlying substrates, it could be evidenced that it must depends also on the thickness of the substrate. As shown in Fig. 5, although the distribution trends are the same for different thickness substrates, the evaporation flux from the droplet surface increases as the thickness of the substrates decreases.

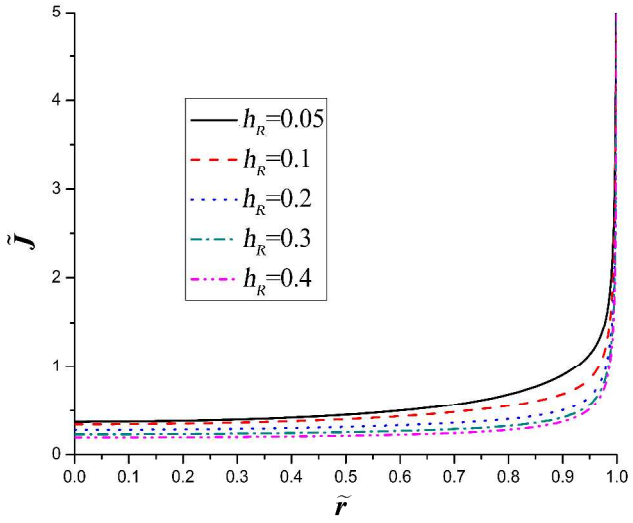

FIG 5 The dimensionless evaporation flux along the surface of sessile droplets at contact angles of 10º computed by the finite element method. The parameters are as follows here: $\tilde{T}_a = 0$, ***Ec*** =10, and k_R=1.5806 for water droplets on glass substrates.

Fig. 6 illustrates that the influences of the substrate thickness on the droplet evaporation also depend on the strength of the evaporative cooling. When the evaporative cooling effect is weak, the substrate thickness has also weak influence on the liquid evaporation. From Fig. 6 it can be seen that, when ***Ec*** is less than 0.2, the relative difference in the evaporation rate between droplets on a substrate with h_R=0.4 and droplets on an isothermal substrate (i.e., h_R =0) is not more than 4.7%. It can also be seen from Fig. 6 that, as the strength of evaporative cooling increases, the decrease in the evaporation rate is more pronounced for thick substrates and the influence of the substrate thickness on the droplet evaporation becomes more and more significant.

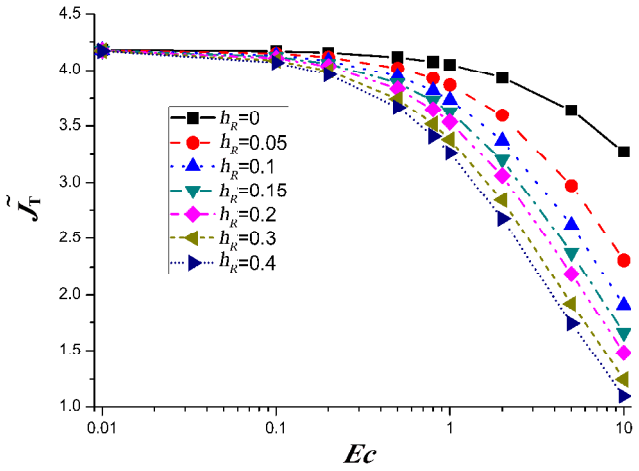

FIG 6 The dimensionless total evaporation rate over the whole surface of sessile droplets at the contact angles of 10° computed by the finite element method. The parameters used are as follows: $\tilde{T}_a = 0$, and k_R=1.5806 for water droplets on glass substrates.

The variations of evaporation rate with h_R for different values of ***Ec*** illustrate more clearly the influence of the evaporative cooling on the effect of the substrate thickness on the droplet evaporation. From Fig. 7a it can be seen that the decrease in the evaporation rate with increasing substrate thickness is more pronounced for the case of stronger evaporative cooling. Here, we define $h_{R,0.95}$ as the relative substrate thickness at which the evaporation rate reduces to 95% of the rate for isothermal substrate. The values of $h_{R,0.95}$ have been measured from Fig. 7a and been plotted against ***Ec*** in Fig. 7b. The numerical results show that $h_{R,0.95}$ is nearly inversely proportional to the evaporative cooling number ***Ec***. In the special case in which there is no evaporative cooling, corresponding to ***Ec***=0, $h_{R,0.95}$ tends to infinity. This means that even a substrate with infinite thickness have no influence on the droplet evaporation if the effect of evaporative cooling can be neglected.

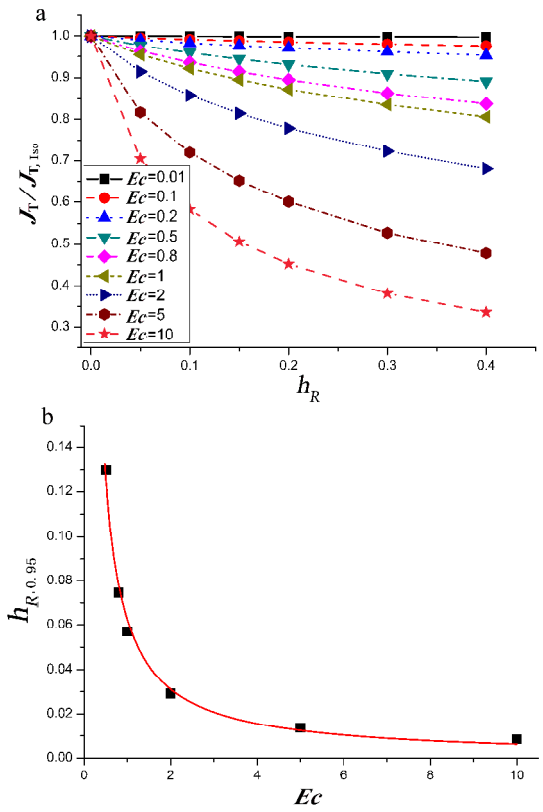

FIG 7 (a) The relative evaporation rate of sessile droplets $J_T/J_{T,Iso}$. Here, $J_{T,Iso}$ is the total evaporation rate for isothermal substrates (i.e., h_R=0). (b) $h_{R,0.95}$ *versus* ***Ec***. The solid squares are from numerical calculations, and the solid line is the fit to the numerical data and yields $h_{R,0.95} = 0.06245/\boldsymbol{Ec}$. The parameters used are as follows: $\tilde{T}_a = 0$, and k_R=1.5806 for water droplets on glass substrates.

C. Effects of the substrate temperature

To investigate the influences of the substrate temperature on the droplet evaporation, the dimensionless evaporation flux $\tilde{J}$ of water droplets on glass substrates with different temperature is illustrated in Fig. 8a. It can be seen from the figure that although the distribution trends are the same for substrates with different temperatures, the evaporation flux from the droplet surface increases remarkably with increasing substrate temperature. Fig. 8b further shows that the total evaporation rate of sessile droplets increases nearly linearly with the substrate temperature.

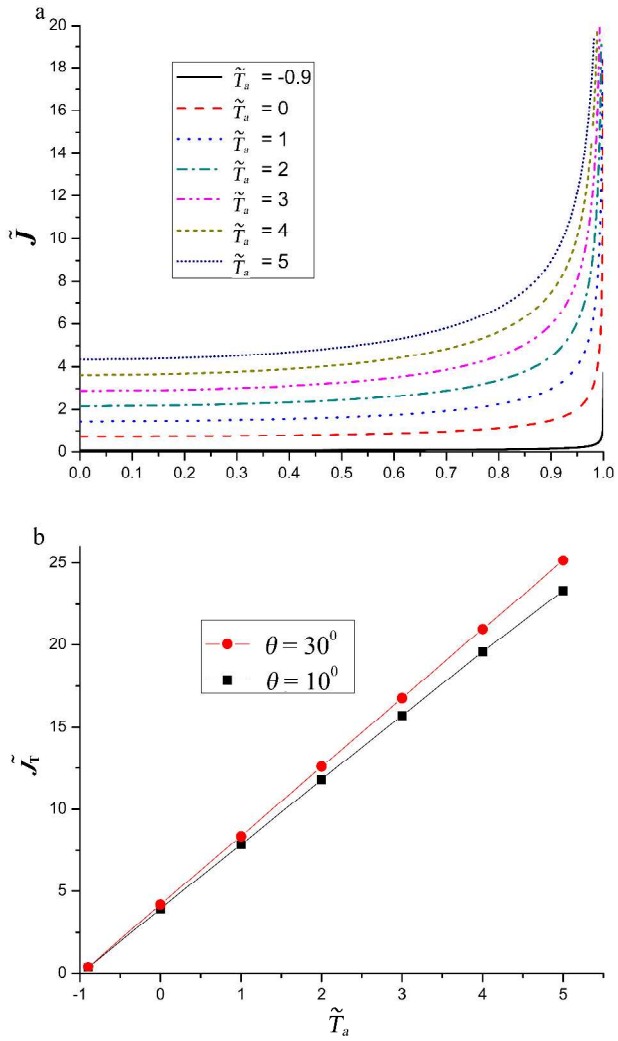

FIG 8 (a) The dimensionless evaporation flux $\tilde{J}$ of drying water droplet on glass substrate computed by the finite element method. Here, the parameters are chosen as follows: ***Ec*** =0.1 (for water droplets drying under an atmospheric pressure), k_R =1.5806 (for water droplets on glass substrates), h_R=0.15, θ=10°, and $\tilde{T}_a$ = -0.9, 0, 1, 2, 3, 4, 5. (b) The dimensionless total evaporation rate $\tilde{J}_T$ of drying water droplets on glass substrates as a function of $\tilde{T}_a$. The parameters used are as follows: h_R =0.15, k_R=1.5806, and ***Ec*** =0.1.

The linear dependence of the evaporation rate on the substrate temperature can be derived theoretically from the equations (1-9). We suppose that $\tilde{T}_1$, $\tilde{T}_2$, and $\tilde{T}_3$ are solutions of the equations (1-9), and $\tilde{T}_{1,0}$, $\tilde{T}_{2,0}$, and $\tilde{T}_{3,0}$ are solutions of the equations for the case $\tilde{T}_a = 0$. We can easily derive that $\tilde{T}_i = \tilde{T}_{i,0}(1+\tilde{T}_a)+\tilde{T}_a$ (i=1, 2, 3), which further gives that $\tilde{J}(\tilde{r}) = \tilde{J}_0(\tilde{r})(1+\tilde{T}_a)$ and $\tilde{J}_T = \tilde{J}_{T,0}(1+\tilde{T}_a)$,

where $\tilde{J}_0$ and $\tilde{J}_{T,0}$ are the dimensionless evaporation flux and the dimensionless total evaporation rate of the case $\tilde{T}_a = 0$ respectively. Then, the function $\tilde{J}(\tilde{r})/(1+\tilde{T}_a) = \tilde{J}_0(\tilde{r})$ along the droplet surface is exactly the same for all the substrate temperatures (see Fig. 9a), and $\tilde{J}_T/\tilde{J}_{T,0} = 1+\tilde{T}_a$ is just a function of $\tilde{T}_a$ (see Fig. 9b). When $\tilde{T}_a = -1$, i.e., $T_a = T_0 - \frac{c_0(1-H)}{b}$, there is no evaporation from the droplet because the vapor concentration above the droplet surface equals to its ambient value far from the droplet.

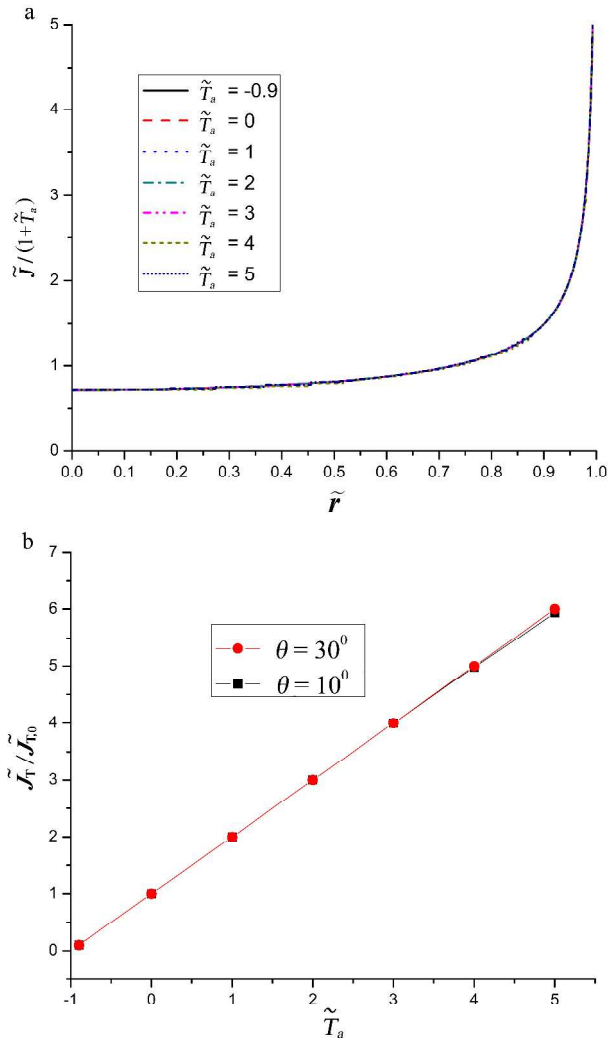

FIG 9 (a) $\tilde{J}/(1+\tilde{T}_a)$ as a function of $\tilde{r}$ at different substrate temperatures, where $\tilde{J}$ is the dimensionless evaporation flux of sessile droplets. The parameters used are as follows: h_R =0.15, k_R

=1.5806, θ=10°, and ***Ec*** =0.1. (b) $\tilde{J}_T/\tilde{J}_{T,0}$ as a function of $\tilde{T}_a$. The parameters used are as follows: h_R =0.15, k_R =1.5806, and ***Ec*** =0.1.

D. Combined effects of substrate and evaporative cooling

Considering the synergy between the evaporative cooling at the droplet surface and the heat conduction across the substrate and the liquid may help to understand the above phenomena. During evaporation, the droplet cools at its free surface due to the latent heat of evaporation. Such evaporative cooling reduces the concentration of vapor at the liquid-air interface, and consequently results in a reduction in the evaporation rate. For the sessile droplets here, the energy required to compensate for the evaporative heat loss and to maintain the evaporation is drawn from the underlying substrate by heat conduction through the substrate and the liquid.

When the effect of the evaporative cooling can be neglected (i.e., ***Ec***=0), the problem of vapor diffusion in the atmosphere is decoupled from the problem of heat transfer in the droplet and the substrate, and accordingly the present model reduces to the basic "isothermal model". In such situation, the vapor concentration field in the surrounding air and the evaporation flux along the droplet surface are determined only by the properties of the liquid and the atmosphere, and thus the substrate has no influence on the droplet evaporation.

If the effect of evaporative cooling is notable, a decrease in the surface temperature will induce a significant reduction in the evaporation rate [50]. Because the heat supply to the droplet surface is closely related to the thermal properties of the substrate, it can thus exert remarkable influences on the evaporation of the droplet. A substrate with a higher thermal conductivity, a smaller thickness, or a higher temperature can supply more heat to the droplet surface, and therefore will result in a higher evaporation rate of the droplet.

The above analysis shows that it is the cooling at the droplet surface and the temperature dependence of the saturation vapor concentration that relate the droplet evaporation to the underlying substrate. The properties of the substrate, including the thermal conductivity, the thickness, and the temperature need to be considered only if the effect of the evaporative cooling must be taken into account. So, the evaporative cooling number ***Ec*** can also be used to identify the influences of the substrate on the droplet evaporation.

E. Comparisons with the experimental results

To verify the validity of the present model, comparisons with the experimental measurements by Dunn et al. [39,40] are performed. Different from the comparisons in ref [50] in which only the data for the perfect thermal conducting substrate (namely, aluminum) were compared, the data for two substrates with the most extreme thermal conductivities (namely, aluminum and PTFE) are used in this paper. In the experiments, three liquids (i.e., water, methanol, and acetone) were used. The ambient atmosphere was air with fixed temperature 295 K, pressure 998 mbar, and relative humidity 0.4 for water and 0 for acetone and methanol.

Fig. 10 shows the comparisons between the experimentally measured values of the evaporation rate of sessile droplets and the theoretical predictions of the present model. For reference, Fig. 10 also includes the theoretical expression of the isothermal model obtained by Hu and Larson [29]. From the figure it can be seen that the present theoretical predictions are in good quantitative agreement with the experimental results, and furthermore are more valid than the isothermal one especially for the thermal insulating substrates. Both the theoretical predictions and the experimental observations demonstrate a linear dependence of the evaporation rate on the droplet radius. Same as the experiments, the present model also reveal the significant difference in the evaporation rate between droplets of the same liquid on different substrates, which is not captured by the isothermal model.

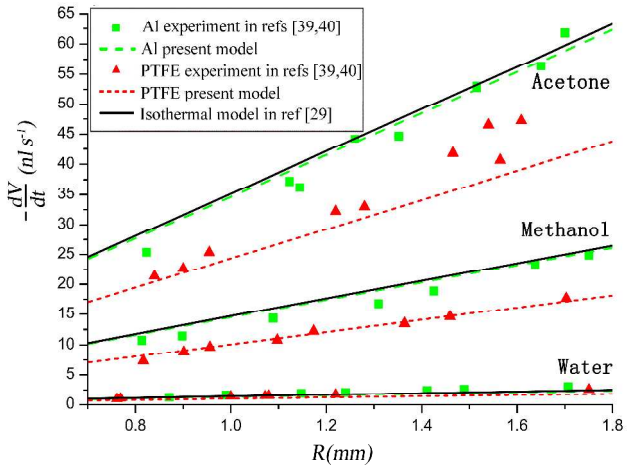

FIG 10 The total evaporation rate for droplets of three liquids on two substrates as a function of the droplet base radius.

Ⅳ. Conclusions

The combined field approach which unifies the coupled physics fields into one single field is first extended, and the thermal properties of the substrate are included in the present model for droplet evaporation. Then, the combined effects of the underlying substrate and the evaporative cooling on the evaporation of sessile droplets have been numerically investigated. We have found that the influence of the substrate on the droplet evaporation depends largely on the strength of the evaporative cooling at the droplet surface. When the evaporative cooling is weak, the substrate has also weak influence on the droplet evaporation. As the strength of evaporative cooling increases, the influence of the substrate on the droplet evaporation becomes more and more significant. The numerical results implied that the evaporative cooling number ***Ec*** can also be used to identify the influence of the substrate on the droplet evaporation.

The combined effects of the underlying substrate and the evaporative cooling on the droplet evaporation have been explained by considering the synergy between the evaporative cooling at the droplet surface and the heat conduction across the substrate and the liquid. The analyses indicated that it

is the cooling at the droplet surface and the temperature dependence of the saturation vapor concentration that relate the droplet evaporation to the underlying substrate. The theoretical predictions of the present model have been compared with previous experimental measurements and found in good agreement without any parameter fitting. Despite its simple origin and limitations, the results presented here may serve as an attempt to understand thoroughly the evaporation process of sessile droplets, and thus may be useful to predict and control the flow field and the deposition pattern of drying droplets.

Acknowledgements

The work is financially supported by the National Natural Science Foundation of China (Grant NO. 51275050), the Program for New Century Excellent Talents in University (Grant NO. NCET-12-0786), and the Specialized Research Fund for the Doctoral Program of Higher Education (Grant NO. 20120014120017).

References

1. R. D. Deegan, Pattern formation in drying drops, Phys. Rev. E, 2000, 61, 475-485.

2. B. M. Weon; J. H. Je, Capillary force repels coffee-ring effect, Phys. Rev. E, 2010, 82, 015305.

3. R. D. Deegan; O. Bakajin; T. F. Dupont; G. Huber; S. R. Nagel; T. A. Witten, Contact line deposits in an evaporating drop, Phys. Rev. E, 2000, 62, 756-765.

4. G. Berteloot; A. Hoang; A. Daerr; H. P. Kavehpour; F. Lequeux; L. Limat, Evaporation of a sessile droplet: Inside the coffee stain, J. Colloid Interface Sci., 2012, 370, 155-161.

5. Y. Cai; B. Z. Newby, Marangoni flow-induced self-assembly of hexagonal and stripelike nanoparticle patterns, J. Am. Chem. Soc., 2008, 130, 6076-6077.

6. T. A. H. Nguyen; M. A. Hampton; A. V. Nguyen, Evaporation of nanoparticle droplets on smooth hydrophobic surfaces: the inner coffee ring deposits, J. Phys. Chem. C, 2013,117 (9), 4707-4716.

7. J. Park; J. Moon, Control of colloidal particle deposit patterns within picoliter droplets ejected by ink-jet printing, Langmuir, 2006, 22, 3506-3513.

8. T. Sekitani; Y. Noguchi; U. Zschieschang; H. Klauk; T. Someya, Organic transistors manufactured using inkjet technology with subfemtoliter accuracy, Proc. Natl. Acad. Sci. U.S.A, 2008, 105, 4976-4980.

9. H. Sirringhaus; T. Kawase; R. H. Friend; T. Shimoda; M. Inbasekaran; W. Wu; E. P. Woo, High-resolution inkjet printing of all-polymer transistor circuits, Science, 2000, 290, 2123-2126.

10. J. R. E. Christy; K. Sefiane; E. Munro, A study of the velocity field during evaporation of sessile water and water/ethanol drops, J. Bionic Eng., 2010, 7, 321-328.

11. M. Schena; D. Shalon; R. W. Davis; P. O. Brown, Quantitative monitoring of gene expression patterns with a complementary DNA microarray, Science, 1995, 270, 467-470.

12. J. P. Jing; J. Reed; J. Huang; X. H. Hu; V. Clarke; J. Edington; D. Housman; T. S. Anantharaman; E. J. Huff; B. Mishra; B. Porter; A. Shenker; E. Wolfson; C. Hiort; R. Kantor; C. Aston; D. C. Schwartz,

Automated high resolution optical mapping using arrayed, fluid-fixed DNA molecules, Proc. Natl. Acad. Sci. U.S.A, 1998, 95, 8046-8051.

13. H. Ghasemi; C. A. Ward, Energy transport by thermocapillary convection during sessile-water-droplet evaporation, Phys. Rev. Lett., 2010, 105, 136102.

14. F. Girard; M. Antoni; K. Sefiane, On the effect of Marangoni flow on evaporation rates of heated water drops, Langmuir, 2008, 24, 9207-9210.

15. H. Ghasemi; C. A. Ward, Mechanism of sessile water droplet evaporation: Kapitza resistance at the solid-liquid interface, J. Phys. Chem. C, 2011, 115, 21311-21319.

16. Y. Hamamoto; J. R. E. Christy; K. Sefiane, Order-of-magnitude increase in flow velocity driven by mass conservation during the evaporation of sessile drops, Phys. Rev. E, 2011, 83, 051602.

17. H. Y. Erbil, Evaporation of pure liquid sessile and spherical suspended drops: A review. Adv. Colloid Interface Sci., 2012, 170, 67-86.

18. K. Sefiane; S. K. Wilson; S. David; G. J. Dunn; B. R. Duffy, On the effect of the atmosphere on the evaporation of sessile droplets of water, Phys. Fluids, 2009, 21, 062101.

19. A. J. Petsi; V. N. Burganos, Temperature distribution inside an evaporating two-dimensional droplet lying on curved or flat substrates, Phys. Rev. E, 2011, 84, 011201.

20. B. Sobac; D. Brutin, Thermocapillary instabilities in an evaporating drop deposited onto a heated substrate, Phys. Fluids, 2012, 24, 032103.

21. K. Zhang; L. R. Ma; X. F. Xu; J. B. Luo; D. Guo, Temperature distribution along the surface of evaporating droplets, Phys. Rev. E, 2014, 89, 032404.

22. X. F. Xu; L. R. Ma; D. D. Huang; J. B. Luo; D. Guo, Linear growth of colloidal rings at the edge of drying droplets, Colloids and Surfaces A: Physicochem. Eng. Aspects, 2014, 447, 28-31.

23. X. F. Xu; J. B. Luo, Marangoni flow in an evaporating water droplet, Appl. Phys. Lett., 2007, 91, 124102.

24. X. F. Xu; J. B. Luo; D. Guo, Radial-velocity profile along the surface of evaporating liquid droplets, Soft Matter, 2012, 8, 5797-5803.

25. T. A. H. Nguyen; A. V. Nguyen, Transient Volume of Evaporating Sessile Droplets: 2/3, 1/1, or Another Power Law?, Langmuir, 2014, 30 (22), 6544-6547.

26. J. M. Stauber; S. K. Wilson; B. R. Duffy; K. Sefiane, On the lifetimes of evaporating droplets, J. Fluid Mech., 2014, 744, R2.

27. T. A. H. Nguyen; A. V. Nguyen, Increased evaporation kinetics of sessile droplets by using nanoparticles, Langmuir, 2012, 28, 16725-16728.

28. X. F. Xu; J. B. Luo; D. Guo, Criterion for reversal of thermal Marangoni flow in drying drops, Langmuir, 2010, 26, 1918-1922.

29. H. Hu; R. G. Larson, Evaporation of a sessile droplet on a substrate, J. Phys. Chem. B, 2002, 106, 1334-1344.

30. R. G. Picknett; R. J. Bexon, Evaporation of sessile or pendant drops in still air, J. Colloid. Interface Sci., 1977, 61, 336-350.

31. R. D. Deegan; O. Bakajin; T. F. Dupont; G. Huber; S. R. Nagel; T. A. Witten, Capillary flow as the cause of ring stains from dried liquid drops, Nature, 1997, 389, 827-829.

32. Y. O. Popov, Evaporative deposition patterns: spatial dimensions of the deposit, Phys. Rev. E, 2005, 71, 036313.

33. H. Hu; R. G. Larson, Marangoni effect reverses coffee-ring depositions, J. Phys. Chem. B, 2006, 110, 7090-7094.

34. H. Hu; R. G. Larson, Analysis of the microfluid flow in an evaporating sessile droplet, Langmuir, 2005, 21, 3963-3971.

35. H. Hu; R. G. Larson, Analysis of the effects of Marangoni stresses on the microflow in an evaporating sessile droplet, Langmuir, 2005, 21, 3972-3980.

36. W. D. Ristenpart; P. G. Kim; C. Domingues; J. Wan; H. A. Stone, Influence of substrate conductivity on circulation reversal in evaporating drops, Phys. Rev. Lett., 2007, 99, 234502.

37. F. Girard; M. Antoni, Influence of substrate heating on the evaporation dynamics of pinned water droplets, Langmuir, 2008, 24, 11342-11345.

38. G. J. Dunn; S. K. Wilson; B. R. Duffy; K. Sefiane, Evaporation of a thin droplet on a thin substrate with a high thermal resistance, Phys. Fluids, 2009, 21, 052101.

39. G. J. Dunn; S. K. Wilson; B. R. Duffy; S. David; K, Sefiane, The strong influence of substrate conductivity on droplet evaporation, J. Fluid Mech., 2009, 623, 329-351.

40. G. J. Dunn; S. K. Wilson; B. R. Duffy; S. David; K, Sefiane, A mathematical model for the evaporation of a thin sessile liquid droplet, Colloids and Surf. A: Physicochem. Eng. Aspects, 2008, 323, 50-55.

41. M. A. Saada; S. Chikh; L. Tadrist, Evaporation of a sessile drop with pinned or receding contact line on a substrate with different thermophysical properties, Int. J. Heat Mass Transf., 2013, 58, 197-208.

42. J. D. Smith; C. D. Cappa; W. S. Drisdell; R. C. Cohen; R. J. Saykally, Raman thermometry measurements of free evaporation from liquid water droplets, J. Am. Chem. Soc., 2006, 128, 12892-12898.

43. S. David; K. Sefiane; L. Tadrist, Experimental investigation of the effect of thermal properties of the substrate in the wetting and evaporation of sessile drops, Colloids and Surfaces A: Physicochem. Eng. Aspects, 2007, 298, 108-114.

44. S. Dash; S. V. Garimella, Droplet evaporation dynamics on a superhydrophobic surface with negligible hysteresis, Langmuir, 2013, 29, 10785-10795.

45. Z. Pan; S. Dash; J. A. Weibel; S. V. Garimella, Assessment of water droplet evaporation mechanisms on hydrophobic and superhydrophobic substrates, Langmuir, 2013, 29, 15831-15841.

46. Z. Pan; J. A. Weibel; S. V. Garimella, Influence of Surface Wettability on Transport Mechanisms Governing Water Droplet Evaporation, Langmuir, 2014, 30, 9726-9730.

47. K. Sefiane; R. Bennacer, An expression for droplet evaporation incorporating thermal effects, J. Fluid Mech., 2011, 667, 260-271.

48. R. G. Larson, Transport and deposition patterns in drying sessile droplets, AIChE J., 2014, 60(5), 1538-1571.

49. N. M. Kovalchuk; A. Trybala; V. M. Starov, Evaporation of sessile droplets, Curr. Opin. Colloid Interface Sci., 2014, 19, 336-342.

50. X. F. Xu; L. R. Ma, Analysis of the effects of evaporative cooling on the evaporation of liquid droplets using a combined field approach, Sci. Rep., 2015, 5, 8614.

51. S. Semenov; V. M. Starov; R. G. Rubio; H. Agogo; M. G. Velarde, Evaporation of sessile water droplets: Universal behaviour in presence of contact angle hysteresis, Colloids and Surfaces A: Physicochem. Eng. Aspects, 2011, 391, 135-144.